

Synthesis, Structure, and Spectroscopic Properties of Ortho-Metalated Platinum(II) Complexes

Millan M. Mdleleni, Jon S. Bridgewater, Richard J. Watts, and Peter C. Ford*

Department of Chemistry, University of California, Santa Barbara, California 93106

Received October 3, 1994[⊗]

The ortho-metalated Pt(II) complexes Pt(ppy)(CO)Cl (**1**), Pt(pty)(CO)Cl (**2**), and Pt(ppy)(Hppy)Cl (**3**) (where ppy and pty are respectively the ortho-C-deprotonated forms of 2-phenylpyridine and 2-*p*-tolylpyridine and Hppy is 2-phenylpyridine) have been prepared. Crystal structure determination performed on a yellow needle of **2** shows that this compound crystallizes in the orthorhombic system, space group *Pna*2₁ (No. 33), with *a* = 7.2025(14) Å, *b* = 19.082(5) Å, *c* = 8.7393(22) Å, *V* = 1201.9(5) Å³, *Z* = 4 molecules/cell, and *R* = 0.046 (*R*_w = 0.056) for 1747 unique reflections. The CO ligand is coordinated *trans* to the nitrogen atom of the ortho-metalated ligand and exerts a strong *trans* effect resulting in a relatively long Pt–N bond [2.114(19) Å]. Characterization of **1** and **2** by IR and ¹H NMR spectra reveals that these complexes have analogous geometries. Complex **3** crystallizes in the monoclinic system, space group *P*2₁/*c* (No. 14), with *a* = 12.023(5) Å, *b* = 9.547(4) Å, *c* = 16.870(7) Å, β = 103.559(5)°, *V* = 1882.5(13) Å³, *Z* = 4 molecules/cell, and *R* = 0.044 (*R*_w = 0.061) for 2361 unique reflections. This structure shows both the bidentate ppy ligand and the monodentate Hppy with the nitrogens of these ligands *trans* to each other. The UV/vis electronic absorption spectra of **1–3** have intense bands in the near-UV region (~375 nm) which have been assigned as metal to ligand charge transfer (MLCT) transitions, and higher energy bands were assigned as ligand-centered transitions. Each complex exhibits relatively long-lived structured emissions in the solid state at ambient temperature and at 77 K and in 77 K glassy toluene solutions. These emissions are proposed to originate from triplet MLCT states. Notably, in solution both the lifetime and spectrum of **2** proved to be a function of the concentration, a phenomenon interpreted in terms of the propensity of square planar d⁸ complexes to oligomerize. In contrast, the more sterically hindered complex **3** displayed no such tendency toward oligomerization.

Introduction

The present study of platinum(II) complexes was initiated as part of continuing investigations in this laboratory concerned with catalytic and photocatalytic activation and functionalization of small molecules.¹ Ortho-metalated complexes of the platinum group elements have been implicated as potential photosensitizers,^{2,3} and the present study was initiated in order to examine the relevant excited states of certain such complexes of platinum(II).

The tendency of transition metal salts to undergo ortho-metalation with heteroaromatic ligands such as 2-phenylpyridine to give five-membered metallocycles has been demonstrated with numerous metals, including Pd(II) and Pt(II).⁴ These are

mostly halo-bridged dimers, although mononuclear cyclometalates of the form M(C[^]N)LX (M = Pd, Pt; C[^]N = ortho-metalated ligand; L = neutral monodentate ligand such as pyridine and phosphines; X = halide) are well documented.⁵ A number of ortho-metalated complexes of the platinum group metals are luminescent,^{2,6,7} and the Pt(II) complexes described here are similarly emissive. An interesting feature of square planar luminophores is a tendency to display multiple emissions attributed in part to the formation of ground state oligomers and excimers.^{8,9} This phenomenon was examined for the present compounds which include two nearly planar complexes with a single cyclometalated phenylpyridine ligand and a third with a second phenylpyridine coordinated in a monodentate fashion. In this case the monodentate ligand is oriented perpendicular to the coordination plane of the Pt(II) in a manner inclined to discourage interplanar stacking.

Described here are the syntheses, structural characterization, spectroscopy, and luminescence properties of the ortho-metalated Pt(II) complexes Pt(ppy)(CO)Cl (**1**), Pt(pty)(CO)Cl (**2**), and Pt(ppy)(Hppy)Cl (**3**) (where ppy and pty are respectively the ortho-C-deprotonated forms of 2-phenylpyridine and 2-*p*-tolylpyridine, and Hppy is 2-phenylpyridine).

[⊗] Abstract published in *Advance ACS Abstracts*, April 1, 1995.

- (1) (a) Wink, D. A.; Ford, P. C. *J. Am. Chem. Soc.* **1987**, *109*, 436. (b) Ford, P. C.; Friedman, A. In *Photocatalysis: Fundamentals and Applications*; Serpone, N., Pelizzetti, E., Eds.; J. Wiley and Sons: New York, 1989; Chapter 16. (c) Ford, P. C.; Netzel, T. L.; Spillett, C. T.; Pourreau, D. B. *Pure Appl. Chem.* **1990**, *63*, 1091. (d) Ford, P. C.; Boese, W.; Lee, B.; McFarlane, K. In *Photosensitization and Photocatalysis Using Inorganic and Organometallic Compounds*; Kalyanasundaram, K., Grätzel, M., Eds.; Kluwer Academic Publishers: Dordrecht, The Netherlands, 1993; pp 359–390. (e) Mdleleni, M. M.; Rinker, R. G.; Ford, P. C. *J. Mol. Catal.* **1994**, *89*, 283. (f) Boese, W. T.; Lee, B. J.; Ryba, D. W.; Belt, S. T.; Ford, P. C. *Organometallics* **1993**, *12*, 4739.
- (2) (a) Ohsawa, Y.; Sprouse, S.; King, K. A.; DeArmond, M. K.; Hanck, K. W.; Watts, R. J. *J. Phys. Chem.* **1987**, *91*, 1047. (b) King, K. A.; Spillane, P. J.; Watts, R. J. *J. Am. Chem. Soc.* **1985**, *107*, 1431.
- (3) Balzani, V.; Bolleta, F.; Ciano, M.; Maestri, M. *J. Chem. Educ.* **1983**, *60*, 447.
- (4) (a) Kasahara, A. *Bull. Chem. Soc. Jpn.* **1968**, *41*, 1272. (b) Cockburn, B. N.; Howe, D. V.; Keating, T.; Johnson, B. F. G.; Lewis, J. J. *Chem. Soc., Dalton Trans.* **1973**, 404. (c) Nonoyama, M.; Takayanagi, H. *Transition Met. Chem.* **1976**, *1*, 10. (d) Caygill, G. B.; Steel, P. J. *J. Organomet. Chem.* **1987**, *327*, 115.

- (5) (a) Weaver, D. L. *Inorg. Chem.* **1970**, *9*, 2250. (b) Gutierrez, M. A.; Newkome, G. R.; Selbin, J. *J. Organomet. Chem.* **1980**, *202*, 341. (c) Vila, J. M.; Gayoso, M.; Pereira, M. T.; Romar, A.; Fernandez, J. J.; Thornton-Pett, M. *J. Organomet. Chem.* **1991**, *401*, 385.
- (6) (a) Chassot, L.; Müller, E.; von Zelewsky, A. *Inorg. Chem.* **1984**, *23*, 4249. (b) Balashev, K. Submitted for publication (personal communication to P.C.F.).
- (7) Chan, C.-W.; Lai, T.-F.; Che, C.-M.; Peng, S.-M. *J. Am. Chem. Soc.* **1993**, *115*, 11245.
- (8) Maestri, M.; Sandrini, D.; von Zelewsky, A.; Deuschel-Cornioley, C. *Inorg. Chem.* **1991**, *30*, 2476.
- (9) Wan, K.-T.; Che, C.-M.; Cho, K. C. *J. Chem. Soc., Dalton Trans.* **1991**, 1077.

Experimental Section

Materials. Tetrabutylammonium chloride, carbon tetrachloride, diethyl ether, ethanol, 2-phenylpyridine, and 2-*p*-tolylpyridine were purchased from Aldrich and were used as received. Dichloromethane, methanol, and acetonitrile were also purchased from Aldrich and were dried and deaerated by standard methods prior to use.¹⁰ Carbon monoxide was purchased from Linde. Potassium tetrachloroplatinate ($K_2[PtCl_4]$) was provided on loan by Johnson-Matthey Inc.

Syntheses of Complexes. The Pt(II) complexes Pt(ppy)(CO)Cl (**1**), Pt(ppy)(CO)Cl (**2**), and Pt(ppy)(Hppy)Cl (**3**) were prepared as follows. The precursor complexes **1** and **2** were either the chloro-bridged dimer $[Pt(C^{\wedge}N)Cl]_2$ ¹¹ or the respective monomer $Bu_4N[Pt(C^{\wedge}N)Cl_2]$ ¹² prepared according to literature methods.

A typical synthesis involved preparing the $(Bu_4N)_2[PtCl_4]$ salt from $K_2[PtCl_4]$ and $[Bu_4N]Cl$ via phase transfer metathesis. The $(Bu_4N)_2[PtCl_4]$ (80 mg, 0.1 mmol) was dissolved in EtOH (20 mL). To this solution was added 1.1 equiv of the phenylpyridine type ligand in CH_2Cl_2 (5 mL). The mixture was allowed to stir at room temperature for 5–7 days, during which time a color change from reddish-brown to light yellow was observed. Reduction of the solution volume followed by addition of Et_2O gave the yellow crystalline dimer $[Pt(C^{\wedge}N)Cl]_2$ in ~65% yield. This material was redissolved in CH_2Cl_2 , and CO was bubbled through the solution at room temperature for 3 h. The result was the formation of cotton-like precipitate which was collected by filtration. Recrystallization from a CH_2Cl_2/Et_2O mixture gave an ~80% yield of **1** or **2** (based on the amount of the precursor used).

Compound **3** was isolated as a minor product during a known, low-yield, synthesis of $Bu_4N[Pt(C^{\wedge}N)Cl_2]$.¹² To a CH_2Cl_2 solution of $(Bu_4N)_2[PtCl_4]$ was added 4 equiv of 2-phenylpyridine in MeOH. The mixture was heated to 50 °C and kept at this temperature for 12 h, during which time shiny yellow-green crystals of $Bu_4N[Pt(C^{\wedge}N)Cl_2]$ were formed. These were isolated in ~30% yield as previously reported.¹² Addition of Et_2O to the filtered reaction solution resulted in precipitation of **3** as a yellow powder that was collected by filtration and recrystallized from CH_2Cl_2/Et_2O , to give yellow parallelepiped crystals in ~10% yield.

Alternative Route. The mononuclear precursor, $Bu_4N[Pt(C^{\wedge}N)Cl_2]$, was prepared in ~30% yield as described above. Bubbling CO through a CH_2Cl_2 solution of this material gave the target complexes in ~80% yield (based on the amount of the precursor used). Complex **1** can also be prepared from **3** by bubbling CO through a CH_2Cl_2 solution of **3** at room temperature. Complex **3** was also prepared in ~85% yield by refluxing a mixture of **1** plus 2 equiv of 2-phenylpyridine in MeOH for 3 h.

Spectroscopic Characterization. The UV/vis electronic absorption spectra were recorded on a Hewlett Packard 8452A diode array spectrophotometer or on an On-Line Instrument Systems (OLIS) modified Cary 118 with 1 cm quartz cells. The extinction coefficients for **1–3** were recorded in CH_2Cl_2 and were reproducible to $\pm 5\%$. The IR spectra were recorded on a Bio-Rad FTS-60 FT-IR spectrometer or on a Mattison 2020 Galaxy Series FT-IR spectrometer. Emission spectra were recorded on a Spex Fluorolog 2 spectrofluorimeter equipped with a water-cooled Hamamatsu R928A photomultiplier tube and were corrected for phototube response. Emission lifetime measurements of both solid and liquid samples were taken on an apparatus based on a Continuum NY 61-20 seeded, Q-switched Nd/YAG laser using the third harmonic ($\lambda = 355$ nm) of the laser beam as the excitation source.¹³ The pulse width of the Nd/YAG laser used in these studies was 10 ns and the energy was 5 mJ/pulse as measured by a

Table 1. Crystal and Refinement Parameters for Pt(ppy)(CO)Cl (**2**) and Pt(ppy)(Hppy)Cl (**3**)

	2	3
formula	$C_{13}H_{10}NOPtCl$	$C_{22}H_{17}N_2PtCl$
fw	426.77	539.93
color	yellow	yellow
habit	needle	parallelepiped
crystal size, mm	$0.6 \times 0.05 \times 0.05$	$0.5 \times 0.5 \times 0.1$
crystal system	orthorhombic	monoclinic
space group	$Pna2_1$ (No. 33)	$P2_1/c$ (No. 14)
<i>a</i> , Å	7.2025(14)	12.023(5)
<i>b</i> , Å	19.082(5)	9.547(4)
<i>c</i> , Å	8.7393(22)	16.870(7)
β , deg	90	103.559(5)
F(000), electrons	785.13	1025.19
Z, molecules/cell	4	
<i>V</i> , Å ³	1201.9(5)	1882.5(13)
ocants collected	$+h, +k, \pm l$	$+h, \pm k, \pm l$
ρ_{calc} , g/cm ³	2.358	1.905
$\lambda(\text{Mo K}\alpha)$, Å	0.710 73	0.710 73
μ , mm ⁻¹	12.00	7.68
range of 2θ , deg	0–60	0–45
scan speed, deg min ⁻¹	4.5	4.5
no. of reflns colcd	2538	5108
no. of unique reflns	1747	2453
R_{merge}	0.054	0.047
no. of obsd reflns, $I > 3\sigma(I)$	1176	2361
transm coeff	0.82–1.00	0.27–1.00
R^a	0.046	0.044
R_w^b	0.056	0.061
<i>S</i>	2.21	3.81

$$^a R = \sum(|F_o| - |F_c|) / \sum |F_o|. \quad ^b R_w = [\sum w(|F_o| - |F_c|)^2 / \sum w F_o^2]^{0.5}; w = 1/[\sigma(F)]^2.$$

Scientech 362 powermeter. The ¹H NMR spectra were recorded on a GN 500 MHz FT-NMR spectrometer in deuterated solvents. The instrument magnet was locked and shimmed to the deuterium signal of the solvent which was also used as an internal reference line.

X-ray Structure Determination. (i) **Complex 2.** Crystals of **2** were grown by slow evaporation of a CH_2Cl_2 solution. A yellow needle of **2** was mounted with epoxy resin on a glass fiber for data collection. X-ray diffraction data were collected at 296 K on a Huber (Crystal-Logic automated) four-circle diffractometer¹⁴ equipped with a graphite-monochromated Mo K α radiation. Lattice parameters were determined by application of the automatic diffractometer indexing routine to the positions of 20 reflections taken from a rotation photograph of the centered crystal in the range $10.0 \leq 2\theta \leq 30.0^\circ$. The diffractometer was operated in the $\theta/2\theta$ scan mode to a maximum 2θ of 60° at a scan rate of $4.5^\circ \text{ min}^{-1}$. Three standard reflections measured after every 97 scans showed no appreciable loss in intensity during the data collection process. Intensity data were empirically corrected for absorption effects by the ψ -scan method. Details of crystal data collection are listed in Table 1.

(ii) **Complex 3.** Yellow parallelepiped crystals of **3** were grown by slow vapor diffusion of Et_2O into a CH_2Cl_2 solution of **3** at room temperature. A good quality crystal of **3** was treated in a manner similar to that for **2**. However, in the case of **3** the unit cell dimensions were obtained from a least-squares refinement of the setting angles of 26 reflections collected in the range $40.0 \leq 2\theta \leq 44.0^\circ$. Three standard reflections measured after every 97 scans showed no appreciable loss in intensity during the data collection process, and an empirical absorption correction (ψ -scans) was performed.

Structure Solution and Refinement. **Complex 2.** The systematic extinctions observed in the reduced data for **2** for $k + l = 2n + 1$ on $0kl$ as well as for $h = 2n + 1$ on $h0l$ were consistent with the $Pna2_1$ (No. 33) and the $Pnma$ (No. 62) space groups. However, solution and refinement of the structure indicated the non-centrosymmetric space

(10) (a) Gordon A. J.; Ford, R. A. *The Chemist's Companion*; John Wiley and Sons: New York, 1972. (b) Perrin, D. D.; Armarego, W. L. F.; Perrin, D. R. *Purification of Laboratory Chemicals*; Pergamon: Oxford, England, 1966.

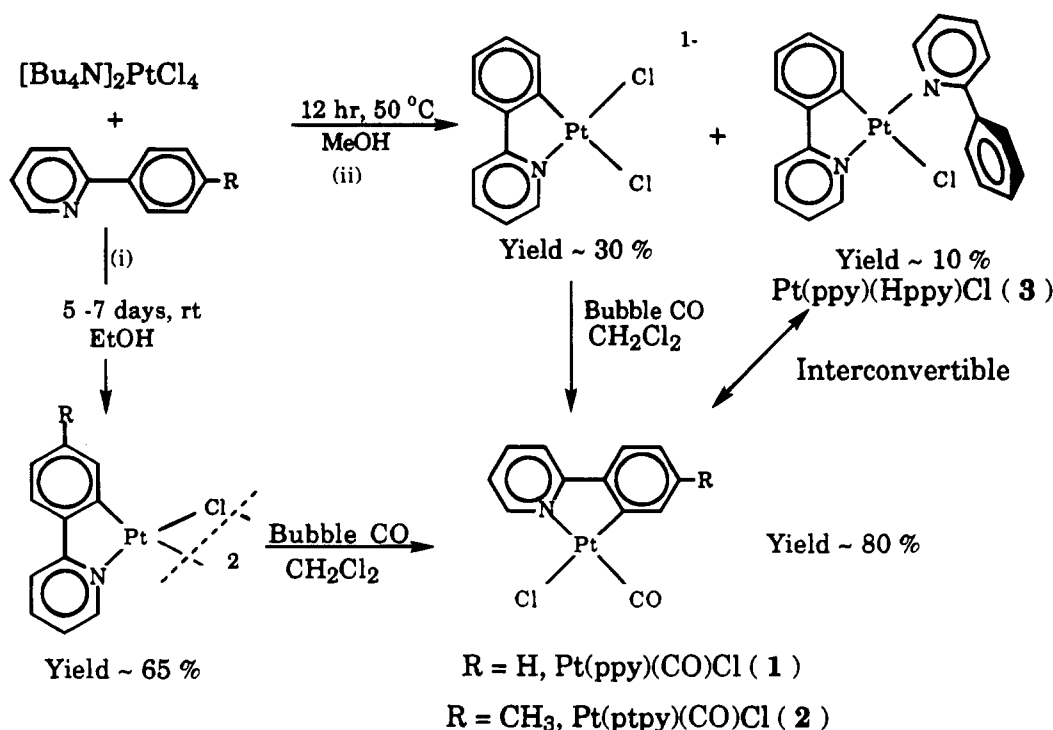
(11) Cope, A.; Siekman, R. W. *J. Am. Chem. Soc.* **1965**, *87*, 3272.

(12) Craig, C. A.; Garces, F. O.; Watts, R. J.; Palmans, R.; Frank, A. J. *Coord. Chem. Rev.* **1990**, *97*, 193.

(13) (a) The system used for lifetime measurements is configured as described previously in ref 13b. However, a Continuum NY 61-20 seeded Q-switched Nd/YAG pulsed laser (pulse width 10 ns) was used in place of the Quanta Ray DCR-1A Q-switched Nd/YAG laser. (b) Kyle, K. R.; Ryu, C. K.; DiBenedetto, J. A.; Ford, P. C. *J. Am. Chem. Soc.* **1991**, *113*, 2954.

(14) The Blake Industries four-circle diffractometer used in these studies consists of a Huber 440 2θ goniometer, a Huber 430 θ goniometer, and a Huber 512 Eulerian Cradle. The diffractometer is interfaced to a DEC micro-VaxII computer with stepping motor controllers from Crystal Logic, Inc.

Scheme 1



group to be the correct choice.¹⁵ The position of the Pt atom in **2** was located by the heavy atom method of SHELXS-86,¹⁶ and the remaining non-hydrogen atoms were located by successive cycles of least-squares refinement and difference Fourier synthesis. Hydrogen atoms were calculated with a C–H distance of 1.08 Å and were refined as riding atoms of their parent atoms. All non-hydrogen atoms were refined anisotropically. The function minimized during full-matrix least-squares refinement was $\sum w(|F_o| - |F_c|)^2$, and the weights were calculated as $w = 1/\sigma^2(F)$. The residuals are given in Table 1; $(\Delta/\sigma)_{\text{max}} = 0.009$; $\Delta\rho_{\text{max,min}} = 4.11, -1.54 \text{ e } \text{Å}^{-3}$, respectively. Scattering factors and anomalous dispersion corrections for scattering factors for non-hydrogen atoms were taken from ref 17. The UCLA Crystallographic Computing Package¹⁸ was used throughout in conjunction with the NRCVAX Crystal Structure Package.¹⁹

Complex 3. The systematic absences observed in the reduced data for **3** for $l = 2n + 1$ on $h0l$, $00l$ and for $k = 2n + 1$ on $0k0$ as well as subsequent least-squares refinement were consistent with the $P2_1/c$ (No. 14) space group. The structure of **3** was solved by the conventional heavy atom method of SHELXS-86 followed by successive cycles of least-squares refinement and difference Fourier synthesis. Hydrogen atoms were included with C–H distance of 1.08 Å in calculated positions and were treated as riding atoms during the course of structure refinement. All non-hydrogen atoms were refined with anisotropic thermal parameters. The residuals are given in Table 1; $(\Delta/\sigma)_{\text{max}} = 0.000$; $\Delta\rho_{\text{max,min}} = 1.75, -2.82 \text{ e } \text{Å}^{-3}$, respectively.

(15) In order to verify that the structure of **2** was refined with the correct direction of the polar axis, parallel refinements were performed with the Roger chirality η fixed at +1 and –1. The R - and R_w factors, respectively, converged to 0.0458 and 0.0561 for η fixed at +1 and to 0.0483 and 0.0593 for η fixed at –1, indicating that the direction of the polar axis was correct. Also, when the chirality η was set at 0 and allowed to refine during the course of structure refinement, the final (refined) chirality η value was 1.15 and the R -factors were $R = 0.0455$ and $R_w = 0.0559$ confirming the correctness of the direction of the polar axis.

(16) Sheldrick, G. M. *SHELXS-86: program for the determination of crystal structures*; University of Gottingen: Gottingen, Germany, 1986.

(17) Cromer, D. T.; Waber, J. T. *International Tables for X-ray Crystallography*; Kynoch Press: Birmingham, U.K., 1974; Vol. IV.

(18) Strouse, C. *The UCLA crystallographic computing package*; Department of Chemistry and Biochemistry, University of California: Los Angeles, CA, 1985.

(19) Gabe, E. J.; Le Page, Y.; Charland, J.-P.; Lee, F. L.; White, P. S. J. *Appl. Crystallogr.* **1989**, *22*, 384.

Results and Discussion

Synthesis. The compounds described in this article can be synthesized in several ways as outlined in Scheme 1. Attempts to prepare the chloro-bridged dimers from K_2PtCl_4 in MeOH/ H_2O or EtOH/ H_2O were unsuccessful; however, use of $(\text{Bu}_4\text{N})_2\text{PtCl}_4$ in MeOH or EtOH as a starting material gave the desired precursor complexes. Allowing the reaction to proceed for a longer period of time (5–7 days) resulted in the formation of the dinuclear ortho-metalated Pt(II) complexes. Since the subsequent reaction was ~80% efficient regardless of which precursor was used, proceeding via dimer formation gives a greater overall efficiency. The preparation of **3** from **1** described in this article is much simpler than that reported earlier, and the overall yields are comparable.¹² Bubbling CO through a CH_2Cl_2 solution of **3** did not lead to the formation of the cationic complex $[\text{Pt}(\text{ppy})(\text{Hppy})\text{CO}]^+$ but slowly gave **1** via the substitution of the pendant 2-phenylpyridine ligand.

Complexes **1–3** are stable to air and are photochemically stable to room light in CH_2Cl_2 . Neither **1** nor **2** shows any detectable CO upon storage in CH_2Cl_2 or in the solid form for several weeks at room temperature.

Infrared Spectra. It has been reported that the bridge-splitting reaction between $[\text{Pd}(\text{Az})\text{Cl}]_2$ (Az = ortho-metalated azobenzene) and pyridine leads to a mixture of isolable *cis* and *trans* isomers.²⁰ However, it appears that only one isomer is formed in each case by the reaction of CO with the halo-bridged Pt(II) complexes $[\text{Pt}(\text{ppy})\text{Cl}]_2$ and $[\text{Pt}(\text{ptpy})\text{Cl}]_2$. The IR spectra of **1** and **2** have sharp single bands in the ν_{CO} region appearing respectively at 2103 and 2102 cm^{-1} in CH_2Cl_2 solution. These relatively high frequencies suggest that the Pt(II) to CO back-bonding is modest, although the ν_{CO} for **1** (2103 cm^{-1} in CH_2Cl_2) is still lower than that for the Pd(II) analog $\text{Pd}(\text{ppy})(\text{CO})\text{Cl}$ (2128 cm^{-1} in CH_2Cl_2).²¹ Although some ortho-metalated Pd(II) complexes have been reported to insert CO into the Pd–C

(20) Grociani, B.; Boschi, T.; Pietropaolo, R.; Belluco, U. *J. Chem. Soc. A* **1970**, 531.

(21) Craig, C. A.; Watts, R. J. *Inorg. Chem.* **1989**, *28*, 309.

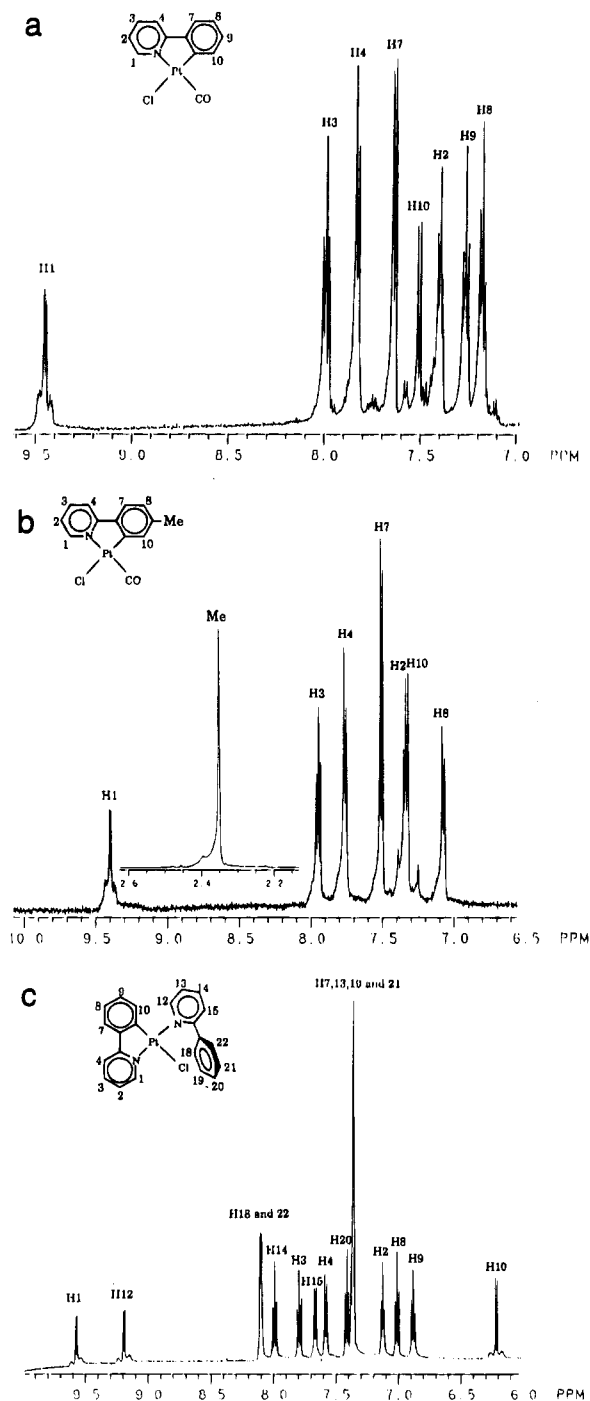


Figure 1. Room-temperature ^1H NMR spectra of $\text{Pt}(\text{ppy})(\text{CO})\text{Cl}$ (a), $\text{Pt}(\text{pty})(\text{CO})\text{Cl}$ (b), and $\text{Pt}(\text{ppy})(\text{Hppy})\text{Cl}$ (c) in CD_2Cl_2 .

σ -bonds when exposed to CO ,^{22,23} there was no effect on the IR spectra of **1** and **2** in CH_2Cl_2 solution when exposed to excess CO for several hours at room temperature.

^1H NMR Spectra. The ^1H NMR spectra of **1–3** in CD_2Cl_2 are shown in Figure 1, and the observed chemical shifts are tabulated in Table 2. Assignments of resonances for **1** and **2** were made through comparison with spectra of the free ligands and of similar compounds.^{5b,24} The aromatic region of the spectrum of **1** has eight well-resolved resonances each integrating for one proton. Four of these are triplets [$\text{H}(2)$, $\text{H}(3)$, $\text{H}(8)$, $\text{H}(9)$] and the other four are doublets [$\text{H}(1)$, $\text{H}(4)$, $\text{H}(7)$, $\text{H}(10)$], as expected for an ortho-metalated phenylpyridinate ligand.

Table 2. Proton NMR Spectroscopic Data for $\text{Pt}(\text{ppy})(\text{CO})\text{Cl}$ (**1**), $\text{Pt}(\text{pty})(\text{CO})\text{Cl}$ (**2**), and $\text{Pt}(\text{ppy})(\text{Hppy})\text{Cl}$ (**3**)^a

resonance ^b	1	2	3
H ₁	9.45 (16.0 Hz) ^c	9.40 (16.2 Hz) ^c	9.58 (20.6 Hz) ^c
H ₂	7.40	7.34	7.13
H ₃	8.00	7.96	7.80
H ₄	7.83	7.76	7.58
H ₇	7.66	7.52	7.36
H ₈	7.18	7.08	7.02
H ₉ /Me	7.27	2.36	6.87
H ₁₀	7.52 (33.5 Hz) ^c	7.32 (30.0 Hz) ^c	6.12 (24.2 Hz) ^c
H ₁₂			9.19 (23.0 Hz) ^c
H ₁₃			7.36
H ₁₄			7.98
H ₁₅			7.67
H ₁₈			8.10
H ₁₉			7.36
H ₂₀			7.42
H ₂₁			7.36
H ₂₂			8.10

^a Chemical shifts were recorded at 298 K in CD_2Cl_2 . ^b Proton assignments are shown in Figure 1, and the labeling used is consistent with numbering scheme used in the crystal structures. ^c The values in parentheses are the $^3J_{\text{Pt-H}}$ coupling constants obtained on a 200 MHz NMR.

Comparison of the resonances of **1** to those of the Pd(II) analog, $\text{Pd}(\text{ppy})(\text{CO})\text{Cl}$,²¹ reveals that more shielding is observed in spectra of the Pt(II) complexes, consistent with observations by Alyea and co-workers.²⁵

The spectrum of **2** has seven resonances in the aromatic region; two of these are triplets [$\text{H}(2)$, $\text{H}(3)$], four are doublets [$\text{H}(1)$, $\text{H}(4)$, $\text{H}(7)$, $\text{H}(8)$], and one is a singlet [$\text{H}(10)$]. The singlet resonance of $\text{H}(10)$ and one triplet of $\text{H}(2)$ are almost superimposed. Each of these resonances integrates for one proton. Another singlet which integrates for three protons is observed upfield (~ 2.38 ppm) and is assigned to the methyl group. Thus, the spectrum is consistent with that expected for an ortho-metalated *p*-tolylpyridinate ligand.

In these complexes, protons ortho to the ligand-binding sites $\text{H}(1)$ and $\text{H}(10)$ show long-range coupling with ^{195}Pt ($I = 1/2$, 34% natural abundance), as evidenced by the occurrence of satellites on either side of their resonances. The $\text{H}(1)$ proton is significantly shifted downfield relative to that of the free ligand, and this can be attributed to the deshielding effect associated with CO in the position *trans* to the pyridyl nitrogen.

The ^1H NMR spectrum of **3** in CD_2Cl_2 has 13 resonances that integrate for a total of 17 aromatic protons in the 6.0–10.0 ppm range as previously reported.¹² Due to its complexity, the assignment of resonances for **3** through comparison with spectra of other ortho-metalated 2-phenylpyridinates was not straightforward. However, use of homonuclear shift correlation spectroscopy (COSY) alleviated the problem. A doublet resonance, flanked by Pt satellites, is observed at 6.20 ppm and is assigned to the $\text{H}(10)$ proton. The X-ray crystal structure of **3** reveals that the $\text{H}(10)$ proton is pointing toward the center of the pyridyl ring of the nonchelated 2-phenylpyridine ligand and, as a consequence, is shielded relative to its counterparts in **1** and **2**. The two doublets that integrate for one proton each observed downfield between 9.0 and 9.80 ppm were assigned to the inequivalent protons $\text{H}(1)$ and $\text{H}(12)$ adjacent to the coordinated nitrogens of the phenylpyridine ligands.

X-ray Crystal Structures. (i) **Complex 2.** Full details of cell parameters, data collection, and final refinement (convergence) data for **2** are summarized in Table 1. The atomic coordinates and the isotropic displacement coefficients, B_{iso} , are listed in Table 3. Table 4 lists the selected bond distances and

(22) Takahashi, H.; Tsuji, J. *J Organomet. Chem.* **1967**, *10*, 511.

(23) Dupont, J.; Pfeffer, M.; Daran, J. C.; Jeannin, Y. *Organometallics* **1987**, *6*, 899.

(24) Chassot, L.; von Zelewsky, A. *Inorg. Chem.* **1987**, *26*, 2814.

(25) Alyea E. C.; Malito, G. *Gazz. Chim. Ital.* **1993**, *123*, 709.

Table 3. Positional and Thermal Parameters^a for Non-Hydrogen Atoms in **2**

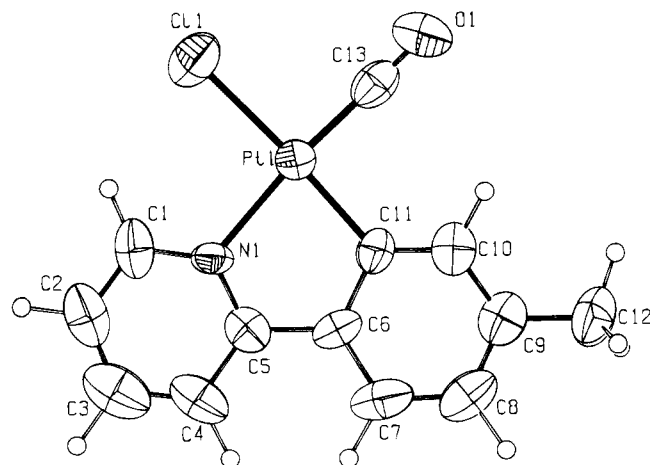
atom	x	y	z	$B_{\text{iso}}, \text{\AA}^2$ ^b
Pt(1)	0.49102(8)	0.73381(3)	0.50343	4.08(3)
Cl(1)	0.5581(11)	0.6494(4)	0.6981(16)	6.8(3)
O(1)	0.560(3)	0.8488(11)	0.7276(24)	6.8(9)
N(1)	0.4297(24)	0.6586(8)	0.3332(24)	3.8(7)
C(1)	0.437(3)	0.5904(11)	0.361(4)	5.8(12)
C(2)	0.388(3)	0.5462(12)	0.243(4)	6.6(13)
C(3)	0.346(3)	0.5707(17)	0.100(4)	7.9(15)
C(4)	0.344(3)	0.6417(14)	0.080(3)	6.2(11)
C(5)	0.3889(24)	0.6866(10)	0.199(3)	4.6(8)
C(6)	0.3859(24)	0.7634(9)	0.195(3)	4.3(8)
C(7)	0.339(3)	0.8007(15)	0.064(3)	6.4(11)
C(8)	0.336(3)	0.8755(13)	0.067(3)	6.1(12)
C(9)	0.386(3)	0.9086(11)	0.203(3)	5.3(10)
C(10)	0.428(3)	0.8688(11)	0.334(3)	4.5(9)
C(11)	0.431(3)	0.7993(10)	0.335(3)	4.5(10)
C(12)	0.381(3)	0.9886(11)	0.201(3)	6.6(12)
C(13)	0.537(3)	0.8044(12)	0.641(4)	5.3(11)

^a Numbers in parentheses are estimated standard deviations in the least significant digit. ^b B_{iso} is the mean of the principal axes of the thermal ellipsoid.

Table 4. Selected Bond Lengths and Angles for Pt(ppy)(CO)Cl (**2**)^a

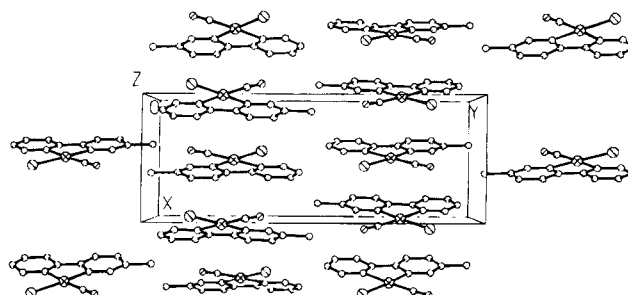
Bond Distances (Å)			
Pt(1)–Cl(1)	2.391(11)	Pt(1)–C(13)	1.84(3)
Pt(1)–N(1)	2.114(19)	C(13)–O(1)	1.15(4)
Pt(1)–C(11)	1.981(24)		
Bond Angles (deg)			
Cl(1)–Pt(1)–N(1)	94.9(5)	C(11)–Pt(1)–N(1)	81.9(9)
Cl(11)–Pt(1)–C(11)	176.8(8)	C(13)–Pt(1)–N(1)	175.5(9)
Cl(1)–Pt(1)–C(13)	89.5(8)	C(11)–Pt(1)–C(13)	93.7(10)

^a Numbers in parentheses are estimated standard deviations in the least significant digits.

**Figure 2.** Molecular structure and numbering of atoms of Pt(ppy)(CO)Cl (**2**). The thermal ellipsoids shown are drawn at the 50% probability level.

angles for **2**. The structure of **2** is depicted in Figure 2, and the packing of the molecules in a unit cell is shown in Figure 3.

There are four molecules of **2** per unit cell. The complex is essentially planar with CO in the coordination site *trans* to the pyridyl nitrogen of the ortho-metallated ligand. Molecular units are slipped-stacked along the "*x/a*" axis, forming chains with average intrachain Pt–Pt separation of 3.66 Å. This Pt–Pt separation is longer than that (3.53 Å) observed in the homoleptic ortho-metallate Pt(ppy)₂.^{6a} Neighboring molecular units are arranged in such a way that the pyridyl ring of one unit lies directly above the phenyl ring of the adjacent unit within a stacked chain.

**Figure 3.** Unit cell contents for Pt(ppy)(CO)Cl (**2**), showing the packing of the molecules.

The narrow N(1)–Pt(1)–C(11) bite angle [81.9(9)°] in **2** is characteristic of ortho-metallated and cyclometallated transition metal complexes.²⁶ All C–C bonds in the phenyl and pyridyl rings show conjugation and the mean C–C distance is 1.39 Å while the C–N bonds of the pyridyl moiety are relatively shorter. The Pt–N bond length [2.114(19) Å] in **2** is slightly longer than those generally observed in similar bipyridyl Pt(II) complexes (e.g. Pt–N distances are 2.033(6) and 2.026(3) Å in [Pt(phen)₂]²⁺,^{26b} and [Pt(bpy)₂]²⁺,^{26c} respectively), indicative of the *trans* effect of the CO ligand. The Pt(1)–C(11) bond distance [1.981(24) Å] is shorter than that observed in the chelated bis(triphenylphosphine) (1,1,3,3-tetracyanopropyl)platinum(II) complex Pt[C₃H₂(CN)₄](PPh₃)₂ [2.138(6) Å]^{27a} and is comparable to that in the bis(phenyl)bis(triphenylphosphine)platinum(II) complex Pt(C₆H₅)₂(PPh₃)₂ [2.033(12) Å].^{27b} The *trans* effect of the phenyl carbon, C(11), bound to the Pt(II) center is marked by the longer Pt–Cl bond length [2.391(11) Å] compared to those in Pt(5,5'-Me₂bpy)Cl₂ (2.295 Å average) and Pt(3,3'-(CH₃OCO)₂bpy)Cl₂ (2.285 Å average)^{28a} or in the yellow (2.291 Å average) and red (2.292 Å average) forms of Pt(bpy)Cl₂.^{28b}

(ii) **Complex 3.** The cell parameters and final refinement data for **3** are given in Table 1. The atomic coordinates and the isotropic displacement coefficients are listed in Table 5, and the selected bond distances and angles are tabulated in Table 6. The molecular structure of **3** is shown in Figure 4, and the unit cell contents are shown in Figure 5.

There are four molecular units of **3** in the unit cell. These are square planar complexes with the nonchelated 2-phenylpyridine ligand bound *trans* to the nitrogen of the pyridyl ring of the ortho-metallated phenylpyridinate ligand. Unlike with **2**, the molecular units of **3** do not stack to form a linear chain, presumably because of steric interactions between pendant phenyl groups as well as the orientation of the Hppy pyridine ring perpendicular to the plane described by the metal-ligand bonds. The Pt–Pt distance between two closest Pt(II) centers is 6.689 Å. The C–C and C–N bonds in both ligands are normal.

The Pt(1)–N(1) and Pt(1)–N(2) bond distances, 2.011(6) Å and 2.032(8) Å, respectively, are similar and are comparable to those observed in Pt(bpy)₂²⁺ and Pt(phen)₂²⁺.^{26b,c} The Pt(1)–C(11) bond length [1.975(8) Å] is similar to that in **2** [1.981-

- (26) (a) Giodano, T. J.; Rasmussen, P. G. *Inorg. Chem.* **1975**, *14*, 1628. (b) Hazell, A. C.; Mukhopadhyay, A. *Acta Crystallogr.* **1980**, *B36*, 1647. (c) Hazell, A.; Simonsen, O.; Wernberg, O. *Acta Crystallogr.* **1986**, *C42*, 1701. (d) Garces, F. O.; Dedeian, K.; Keder, N.; Watts, R. J. *Acta Crystallogr.* **1993**, *C49*, 1117. (e) Stoccoro, S.; Cinellu, M. A.; Zucca, A.; Minghetti, G.; Cernatin, F. *Inorg. Chim. Acta* **1994**, *215*, 17.
- (27) (a) Yarrow, D. J.; Ibers, J. A.; Lenarda, M.; Graziani, M. *J. Organomet. Chem.* **1974**, *70*, 133. (b) Debaerdemaeker, T.; Klein, H.-P.; Wiege, M.; Brune, H. A. *Z. Naturforsch.* **1981**, *36B*, 958.
- (28) (a) Miskowski, V. M.; Houlding, V. H.; Che, C.-M.; Wang, Y. *Inorg. Chem.* **1993**, *32*, 2518. (b) Herber, R. H.; Croft, M.; Coyer, M. J.; Bilash, B.; Sahiner, A. *Inorg. Chem.* **1994**, *33*, 2422.

Table 5. Positional and Thermal Parameters^a for Non-Hydrogen Atoms in **3**

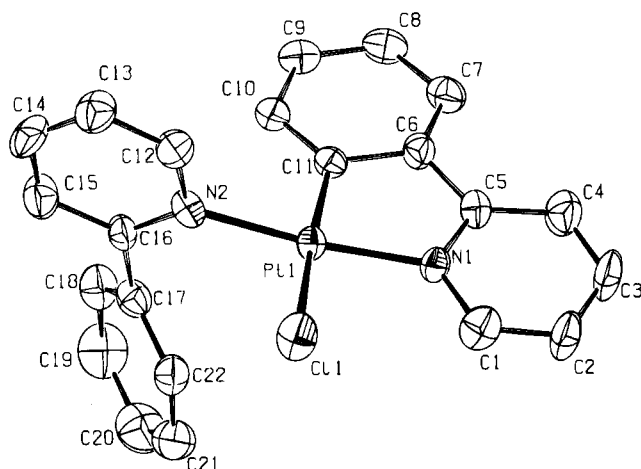
atom	x	y	z	$B_{iso}, \text{\AA}^2$ ^b
Pt(1)	0.23367(3)	0.05092(3)	0.149787(17)	2.153(20)
Cl(1)	0.16504(21)	0.1137(3)	0.00809(13)	3.67(11)
N(1)	0.0992(6)	0.1314(6)	0.1861(4)	2.2(3)
N(2)	0.3797(7)	-0.0223(7)	0.1236(4)	2.6(3)
C(1)	-0.0013(8)	0.1721(9)	0.1365(5)	3.4(4)
C(2)	-0.0863(8)	0.2355(10)	0.1656(6)	3.8(4)
C(3)	-0.0684(9)	0.2630(11)	0.2478(6)	4.0(5)
C(4)	0.0314(9)	0.2173(10)	0.2992(6)	3.9(5)
C(5)	0.1145(7)	0.1478(8)	0.2682(5)	2.5(3)
C(6)	0.2185(8)	0.0809(8)	0.3167(5)	2.5(4)
C(7)	0.2421(9)	0.0699(9)	0.4017(6)	3.0(4)
C(8)	0.3391(9)	-0.0083(10)	0.4421(5)	3.1(4)
C(9)	0.4057(8)	-0.0753(9)	0.3968(5)	3.0(4)
C(10)	0.3805(8)	-0.0631(7)	0.3108(5)	2.5(4)
C(11)	0.2874(8)	0.0158(8)	0.2680(5)	2.2(4)
C(12)	0.4606(9)	0.0782(10)	0.1182(6)	3.4(4)
C(13)	0.5691(9)	0.0440(9)	0.1085(7)	3.5(5)
C(14)	0.5965(8)	-0.0950(12)	0.1043(6)	3.9(5)
C(15)	0.5169(9)	-0.1971(9)	0.1095(6)	3.6(4)
C(16)	0.4069(7)	-0.1588(9)	0.1183(5)	2.4(3)
C(17)	0.3192(8)	-0.2671(9)	0.1184(5)	2.8(4)
C(18)	0.3511(9)	-0.3891(10)	0.1670(5)	3.6(4)
C(19)	0.2741(12)	-0.4957(12)	0.1636(7)	4.7(6)
C(20)	0.1645(13)	-0.4883(14)	0.1126(8)	4.9(6)
C(21)	0.1338(9)	-0.3694(10)	0.0636(6)	3.8(5)
C(22)	0.2102(8)	-0.2592(9)	0.0678(5)	3.1(4)

^a Numbers in parentheses are estimated standard deviations in the least significant digit. ^b B_{iso} is the mean of the principal axes of the thermal ellipsoid.

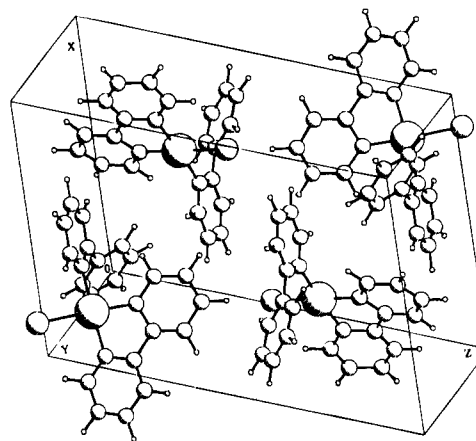
Table 6. Selected Bond Lengths and Angles for Pt(ppy)(Hppy)Cl (**3**)^a

Bond Distances (Å)			
Pt(1)–Cl(1)	2.4145(23)	Pt(1)–N(2)	2.032(8)
Pt(1)–N(1)	2.011(6)	Pt(1)–C(11)	1.975(8)
Bond Angles (deg)			
Cl(1)–Pt(1)–N(1)	95.39(18)	N(1)–Pt(1)–N(2)	174.2(3)
Cl(1)–Pt(1)–N(2)	88.99(21)	N(1)–Pt(1)–C(11)	81.6(3)
Cl(1)–Pt(1)–C(11)	175.24(25)	N(2)–Pt(1)–C(11)	93.8(3)
Torsion Angles (deg)			
C(12)–N(2)–Pt(1)–C(11)			95.5(6)
N(2)–C(16)–C(17)–C(22)			49.2(6)

^a Numbers in parentheses are estimated standard deviations in the least significant digits.

**Figure 4.** Molecular structure and numbering of atoms of Pt(ppy)(Hppy)Cl (**3**). The thermal ellipsoids shown are drawn at the 50% probability level. Hydrogen atoms are omitted for clarity.

(24 Å). The relatively long Pt(1)–Cl(1) bond length [2.415(2) Å] is a reflection of the strong *trans* effect of the coordinated carbon, C(11) of the ortho-metalated ligand. The bite angle,

**Figure 5.** Unit cell contents for Pt(ppy)(Hppy)Cl (**3**), showing the packing of the molecules as well as the relatively long Pt–Pt separation.

N(1)–Pt(1)–C(11) [81.6(3)°] is similar to that observed in **2** [81.9(9)°]. The phenyl and the pyridyl rings of the ortho-metalated phenylpyridine ligand have an angle of 2.7(4)° between their planes.

The torsion angle C(12)–N(2)–Pt(1)–C(11) [95.5(6)°] indicates that the pyridyl ring of the nonchelated 2-phenylpyridine ligand is almost perpendicular to the plane of the molecule. The Hppy pyridyl ring is oriented such that the H(10) proton of ppy is pointing directly at its center, leading to the effect on the ¹H NMR chemical shift of H(10) discussed above. The phenyl ring of the nonchelated 2-phenylpyridine ligand is twisted by 49.2(6)°, about the inter-ring C(15)–C(16) bond, relative to the pyridyl ring of the same ligand. This complex is one of several Pt(II) complexes containing a chelated and a nonchelated ortho-metalating ligand whose crystal structures have been successfully determined.^{26a,e}

Due to twinning, the crystal structure of **1** has not yet been satisfactorily determined. However, indexing of its powder diffraction pattern shows it to be monoclinic with $a = 8.889$ Å, $b = 9.139$ Å, $c = 17.010$ Å, $\beta = 102.74^\circ$, and $V = 1347.8$ Å³. On the basis of the proton NMR results, it is believed that the arrangement of ligands around the Pt(II) center in **1** is analogous to that observed in **2**.

Electronic Absorption Spectra. The electronic absorption spectral data for **1–3** in various organic solvents are presented in Table 7, and the spectra in dichloromethane are shown in Figures 6–8, respectively. Previously^{12,24,29} bands in the near-UV region of the electronic absorption spectra of ortho-metalated 2-phenylpyridine complexes of Pt(II) have been assigned to metal to ligand charge transfer (MLCT) transitions, and an analogous assignment appears appropriate here. This would be consistent with the modest solvent sensitivity of the longest wavelength bands of **1–3** (Table 7) and the blue shift of this band from that seen for Pt(ppy)Cl₂[–] (λ_{max} 379 nm) when a π -donor Cl[–] is replaced by a π -acceptor CO to give Pt(ppy)(CO)Cl (λ_{max} 372 nm). Unlike **1** and **2**, complex **3** has two bands in the near-UV region. These are at 384 and 402 nm in CH₂Cl₂. The band at 402 nm has been previously assigned as MLCT.¹² In this case, the transition is likely to be to the π^* orbital of the uncharged monodentate ligand. Another MLCT band appears at λ_{max} (384 nm) similar to those seen for **1** and **2**.

The UV bands observed in the absorption spectra of **1** and **2** can be attributed to ligand-centered (LC) π – π^* transitions perturbed by complexation to the Pt(II) center. Given the relatively high field strengths of the carbonyl and the ortho-

(29) Maestri, M.; Sandrini, D.; Balzani, V.; Chassot, L.; Jolliet, P.; von Zelewsky, A. *Chem. Phys. Lett.* **1985**, *122*, 375.

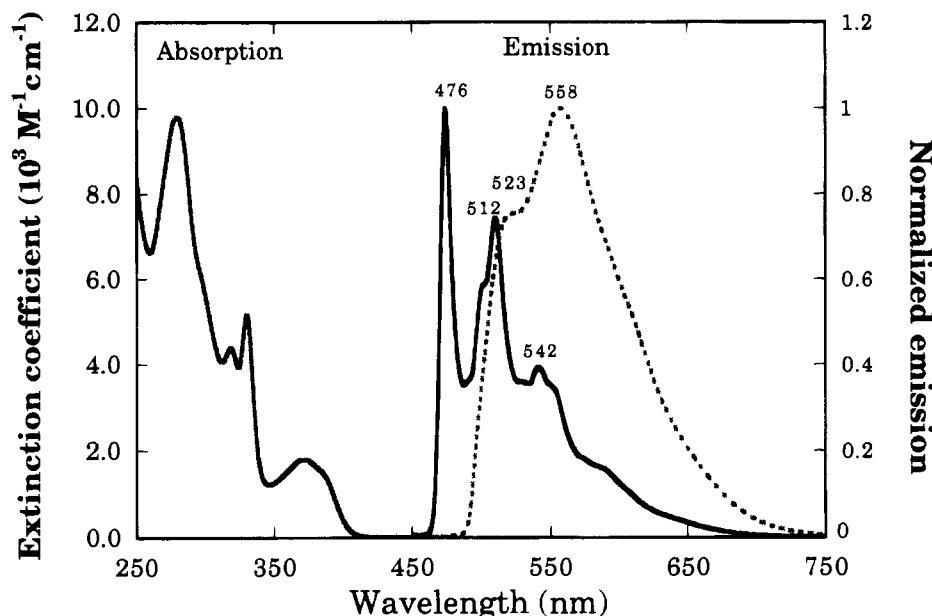


Figure 6. Room-temperature UV/vis absorption spectrum (left) in CH_2Cl_2 and the 77 K emission spectra (right) of $\text{Pt}(\text{ppy})(\text{CO})\text{Cl}$ (**1**) in dilute toluene (10^{-6} M) glass (—) and in the solid state (---).

Table 7. UV/Vis Absorption Features and Extinction Coefficients for **1-3** in Various Organic Solvents

compound	λ_{max} (nm)			extinction coeff ($10^3 \text{ M}^{-1} \text{ cm}^{-1}$) ^a
	CH_3CN	CH_2Cl_2	CCl_4	
$\text{Pt}(\text{ppy})(\text{CO})\text{Cl}$	276	280	286	9.8
	294 (sh)	296 (sh)	300 (sh)	6.3
	316	318	320	4.5
	328	330	332	5.1
	367	372	380	2.0
	367	372	380	2.0
$\text{Pt}(\text{ptpy})(\text{CO})\text{Cl}$	282	284	289	10.6
	296 (sh)	298 (sh)	302 (sh)	7.7
	321	324	325	4.3
	332	334	338	5.3
	372	378	383	2.3
	<i>b</i>	<i>b</i>	<i>b</i>	<i>b</i>
$\text{Pt}(\text{ppy})(\text{Hppy})\text{Cl}$	254	260	<i>b</i>	28.7
	276 (sh)	280 (sh)	282 (sh)	18.1
	310 (sh)	314 (sh)	314 (sh)	7.6
	324 (sh)	328 (sh)	328	5.8
	346	348	356	4.1
	380 (sh)	384	394	2.3
	400	402	416	2.1
	<i>b</i>	<i>b</i>	<i>b</i>	<i>b</i>
2-phenylpyridine	248	248	<i>b</i>	13.6
	276	276	278	10.9
2- <i>p</i> -tolylpyridine	254	256	<i>b</i>	13.3
	278	280	282	12.2

^a Extinction coefficients were measured in CH_2Cl_2 to an experimental reproducibility of $\pm 5\%$. ^b Could not be taken reliably due to solvent cutoff.

metalating ligands in **1-3**, metal-centered ligand field (LF) bands of **1-3** are also expected to be in the UV region. However, due to the small extinction coefficients associated with d-d transitions, these would be easily masked by the ligand-centered $\pi-\pi^*$ bands and / or the MLCT bands.

Emission Spectra. Excitation of **1-3** at their lowest energy absorption bands (λ_{ex} 350–400 nm) resulted in structured emissions with vibrational progressions of 1000–1500 cm^{-1} . At 298 K, compounds **1** and **2** are luminescent only in the solid state while **3** is emissive in the solid state and in solution, though the emission is weak in the latter case. At 77 K, **1-3** are emissive in the solid state as well as in glassy solutions. The 77 K emission spectra of dilute solutions (10^{-6} M) of **1-3** in toluene and as solids are shown in Figures 6–8, respectively. Structured emission spectra are commonly observed when the

emitting excited states are LC or MLCT in character.³⁰ The criteria generally used to differentiate between these two types of lowest ES are drawn from an evaluation of lifetime data and of solvent effects on the energies and structure, of the emission maxima compared to those of the free ligand. The band maxima of **1-3** show some modest sensitivity to the solvent consistent with a MLCT assignment. Comparison of these with emission spectra of the free ligands reveals that the spectra of the complexes are quite different and display $E^{\circ\circ}$ values from 1900 to 2400 cm^{-1} lower than of the respective free ligand.

The emission lifetimes of **1-3** as solids and in dilute solutions (1.0 μM) are given in Table 8. Single-exponential decays were observed in each of these cases. The ~ 30 μs lifetimes of **1** and **2** in 77 K toluene glasses are shorter than generally expected for LC emissions but somewhat longer than lifetimes usually associated with emissions from MLCT excited states in heavy metal complexes. This suggests that there may be some mixing of the LC and MLCT states as proposed for a $\text{Rh}(\text{III})-2$ -phenylpyridine complex³¹ and in other ortho-metalates.³²

Toluene solutions of **3** were seen to be weakly emissive at room temperature and much more strongly emissive at 77 K. The emission lifetimes of 641 ns at 298 K and 11.2 μs at 77 K would be consistent with a ³MLCT assignment of the emitting state.

Both **1** and **2** show marked differences between emission spectra recorded in the solid state and dilute glassy solutions at 77 K. The solid state emissions are red shifted and are less structured. Variation of the emission structure with Pt–Pt intermolecular separation in $\text{Pt}(\text{II})$ complexes is a well documented phenomenon.³³ The Pt–Pt separation of 3.66 Å in **2** is on the upper end of the range (3.4–3.7 Å)^{33b} associated with $\text{Pt}(\text{II})$ dimers. Thus, weak interactions between two adjacent

(30) (a) Crosby, G. A. *Acc. Chem. Res.* **1975**, *8*, 231. (b) Crosby, G. A. *J. Chem. Educ.* **1983**, *60*, 791.

(31) Maestri, M.; Sandrini, D.; Balzani, V.; Maeder, U.; von Zelewsky, A. *Inorg. Chem.* **1987**, *26*, 1323.

(32) (a) Zilian, A.; Maeder, U.; Güdel, H. U. *J. Am. Chem. Soc.* **1989**, *111*, 3855. (b) Colombo, M. G.; Hauser, A.; Güdel, H. U. *Inorg. Chem.* **1993**, *32*, 3088.

(33) (a) Miskowski, V. M.; Houlding, V. *Inorg. Chem.* **1991**, *30*, 4446. (b) Houlding, V.; Miskowski, V. M. *Coord. Chem. Rev.* **1991**, *111*, 145. (c) Bailey, J. A.; Miskowski, V. M.; Gray, H. B. *Inorg. Chem.* **1993**, *32*, 369.

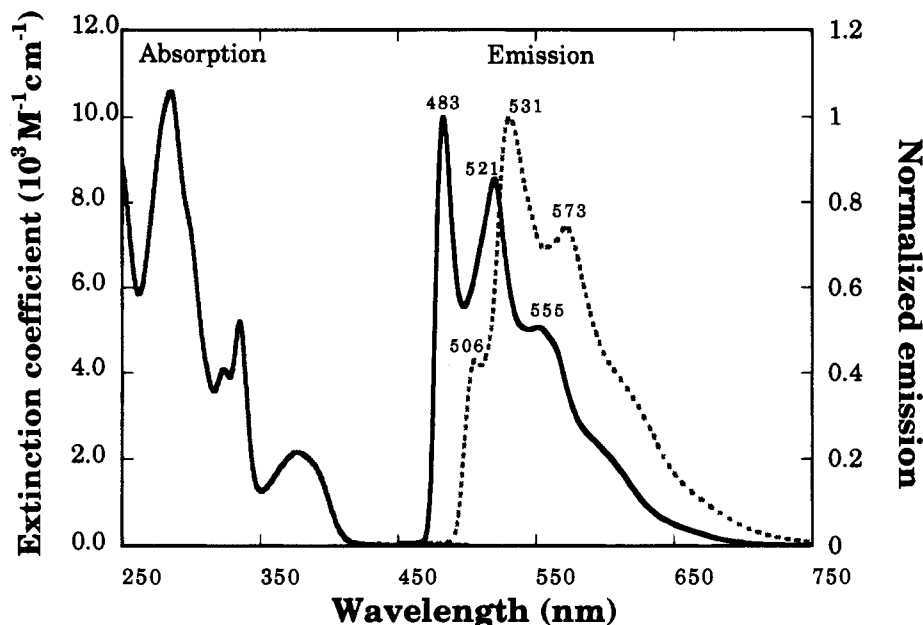


Figure 7. Room-temperature UV/vis absorption spectrum (left) in CH_2Cl_2 and the 77 K emission spectra (right) of $\text{Pt}(\text{ppy})(\text{CO})\text{Cl}$ (**2**) in dilute toluene (10^{-6} M) glass (—) and in the solid state (---).

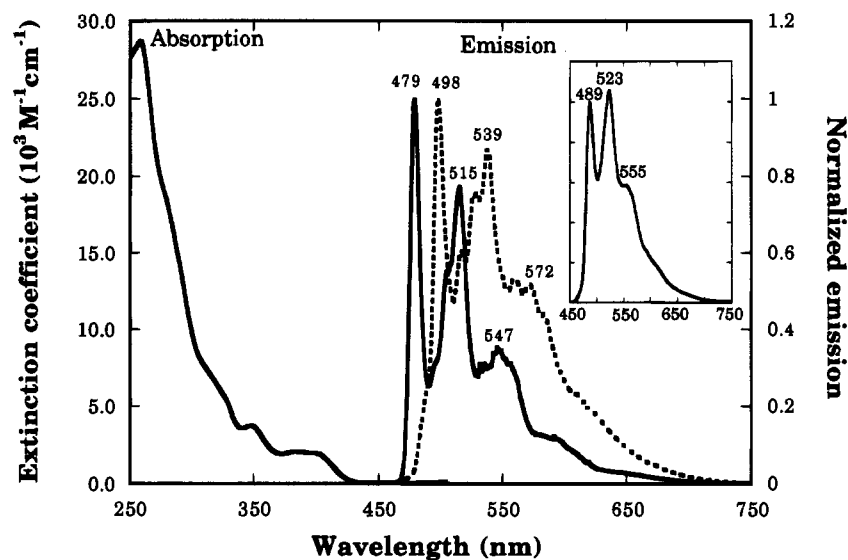


Figure 8. Room-temperature UV/vis absorption spectrum (left) in CH_2Cl_2 and the 77 K emission spectra (right) of $\text{Pt}(\text{ppy})(\text{Hppy})\text{Cl}$ (**3**) in toluene glass (—) and in the solid state (---). Inset: Normalized emission spectrum of $\text{Pt}(\text{ppy})(\text{Hppy})\text{Cl}$ (**3**) in 298 K toluene.

Table 8. Luminescence Data for $\text{Pt}(\text{ppy})(\text{CO})\text{Cl}$ (**1**), $\text{Pt}(\text{ppy})(\text{CO})\text{Cl}$ (**2**), and $\text{Pt}(\text{ppy})(\text{Hppy})\text{Cl}$ (**3**)^a

complex	lifetime (λ_{max}) ^b			
	solid, 298 K	solid, 77 K	soln, 298 K	soln, 77 K
$\text{Pt}(\text{ppy})(\text{CO})\text{Cl}$	1.1 μs (528 nm)	3.5 μs (523 nm)		28 μs (476 nm)
$\text{Pt}(\text{ppy})(\text{CO})\text{Cl}$	959 ns (510 nm)	6.1 μs (506 nm)		32 μs (483 nm)
$\text{Pt}(\text{ppy})(\text{Hppy})\text{Cl}$	473 ns (505 nm)	6.9 μs (498 nm)	641 ns (489 nm)	11.2 μs (479 nm)
2-phenylpyridine				> 100 ms (430 nm) ^c
2- <i>p</i> -tolylpyridine				> 100 ms (442 nm) ^d

^a Emission spectra and lifetime measurements were taken in toluene or in the solid state. ^b Highest energy feature of the luminescence emission maxima. ^c In propionitrile/butyronitrile (4/5, v/v) glass, from ref 31. ^d In butyronitrile glass.

$\text{Pt}(\text{II})$ centers may be occurring in solid **2** and presumably in solid **1**. At such intermediate distances, weak interactions between the π -orbitals of the ortho-metalated ligands on adjacent molecules may also be important to the spectroscopy.

Such intercomplex interactions generally lead to excimeric emissions that are characterized by Gaussian-shaped emission bands in complexes with shorter Pt–Pt separations.^{6a,33} In agreement with this interpretation, the differences between the solid state and the dilute frozen glass solution emission spectra

of **3** at 77 K were less dramatic, albeit the former is red-shifted compared to the latter. The much longer Pt–Pt internuclear distances in the solids of **3** preclude Pt–Pt interactions in the ground and excited states. Furthermore, the absence of coplanar stacking of π -unsaturated ligands argues against significant π -interactions between adjacent molecular units.

In an effort to test the validity of the above argument, concentration dependence studies were undertaken using complexes **2** and **3**. The 77 K emission spectra of **3** in toluene

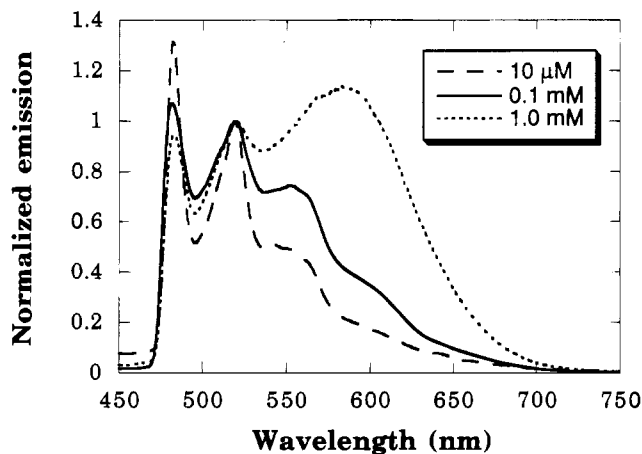


Figure 9. Concentration dependence of the emission spectrum of **2** in toluene at 77 K: 10^{-5} M (---); 10^{-4} M (—); 10^{-3} M (···). The spectra were normalized to the 521 nm band.

solutions were unchanged as the concentration of **3** was varied from $1.0 \mu\text{M}$ to 1.0 mM . This observation is in keeping with the rationale that intermolecular interactions are unfavorable for **3** owing to steric interactions of the Hppy ligand. However, analogous 77 K solutions of **2** showed changes in the emission over the $1.0 \mu\text{M}$ – 1.0 mM range (Figure 9). A Gaussian-shaped band grew in at 585 nm at the expense of the 483 nm band as the solution concentration was increased. The resulting spectra at higher concentration are similar to but not identical with those seen for the solids (Figures 6 and 7), and a logical conclusion is that this results from formation of dimeric or oligomeric species in solution. It has been previously shown that a new low-energy band(s), attributed to the formation of oligomers, appears in the emission spectra of square planar Pt(II) complexes upon an increase in solution concentration or upon application of pressure to the system.³⁴ In the present studies, a plot of $\log(I_{585}/I_{483})$ vs $\log[2]$ (where I_{585}/I_{483} is the ratio of the intensity of the 585 nm band to that of the band at 483 nm at 77 K) shows that such dimeric or oligomeric species are spectroscopically significant only when $[2]$ is greater than $50 \mu\text{M}$.

Emission lifetime measurements were also taken for 77 K toluene solutions of **2** in the $1.0 \mu\text{M}$ – 1.0 mM range. Monoexponential decays were observed for solutions of concentration $<0.1 \text{ mM}$, and the lifetime was found to be $32 \mu\text{s}$, independent of concentration. However, at higher concentrations of **2**, the emission decay curves could not be represented by simple single-exponential functions but could only be fit as a sum of two or more exponential functions. The fast component of the emission decay curve gave an average lifetime of $6.5 \mu\text{s}$, and the slow component gave lifetimes ($30.6 \mu\text{s}$) similar to those of the dilute solutions.³⁵ Thus, both the emission spectra and the temporal emission decay properties indicate oligomer formation for **2** in concentrations $>10^{-4} \text{ M}$ under these conditions.

(34) (a) Schindler, J. W.; Fukuda, R. C.; Adamson, A. W. *J. Am. Chem. Soc.* **1982**, *104*, 3595. (b) Lechner, A.; Gliemann, G. *J. Am. Chem. Soc.* **1989**, *111*, 7469. (c) Kunkely, H.; Vogler, A. *J. Am. Chem. Soc.* **1990**, *112*, 5625.

Photochemical Observations. When CH_2Cl_2 solutions of **1** were irradiated with light of $\lambda > 350 \text{ nm}$ (from a high-pressure Hg lamp) under Ar, the only reaction observed was the photoejection of CO with concurrent formation of the chloro-bridged dimer $[\text{Pt}(\text{ppy})\text{Cl}]_2$. The extent of dimerization was reduced when the reaction was performed under CO. However, quantum yields were not determined.

Summary

The X-ray crystal structure determinations of **2** and **3** revealed that CO and unchelated 2-phenylpyridine are respectively bound *trans* to the nitrogen of the coordinated ortho-metalated ligand. Due to the strong σ -donor ability of 2-phenylpyridine, the electronic spectra of these complexes have MLCT bands located in the near-UV region, the energies of which are a function of the ligand field strengths as well as the π -acceptor abilities of the ligands bound to the Pt(II) center. The 77 K emission spectra of these complexes show some dependence on the packing of the molecular units and the Pt–Pt separations in the solid state. Compounds **1** and **2** with short metal–metal separations and linear-chain structures exhibit less structured emission spectra compared to compound **3** with long Pt–Pt separations. Furthermore, the emission spectra of toluene solutions of **2** at 77 K display marked concentration dependence in the $1.0 \mu\text{M}$ – 1.0 mM range, an observation attributed to the stacking of molecular units in oligomers at higher concentrations. The lifetime of the oligomers of **2** is about $6.5 \mu\text{s}$ at 77 K. In contrast, no such intermolecular interactions were suggested by concentration studies of luminescence from compound **3**. The emitting states in these complexes have been assigned as being $^3\text{MLCT}$ in character.

Acknowledgment. This research was supported by a grant (DE-FG03-85ER13317) to P.C.F. from the Division of Chemical Sciences, Office of Basic Energy Research, U.S. Department of Energy. The nanosecond laser (described in ref 13) utilized in these studies was provided by a DOE URI grant (DE-FG05-91ER79039) to P.C.F. M.M.M. thanks UCSB and the United Nations (UNETPSA) for a tuition fellowship and a stipend fellowship, respectively. The crystallographic assistance provided by Dr. Xianhui Bu of this department is appreciated. The platinum used in these studies was provided on loan by Johnson-Matthey, Inc. Preliminary studies on related compounds were carried out in this laboratory by Jon Songsted.

Supplementary Material Available: Full tables listing anisotropic thermal parameters for non-hydrogen atoms, atomic coordinates for hydrogens, and bond lengths and angles for **2** and **3** (Tables S-1 to S-6) (9 pages). Ordering information is given on any current master-head page.

IC941127Q

(35) It is interesting to note that the lifetime of the fast component is similar to that of the solid at 77 K. At a glance, this observation suggests the possibility of crystallizing some of **2** out of the solution as the temperature is lowered from room temperature to 77 K. However, the absence of the intense band at 531 nm that is characteristic of the solid emission at 77 K dispelled such doubts.